דו"ח מדעי מסכם לתכנית מחקר מספר 20-07-0027

שנת המחקר: 3 מתוך 3 שנים

פיתוח ביוסנסור אלקטרוכימי לזיהוי וכימות מהיר של רעלנים המיוצרים על ידי חיידקים כחוליים במאגרי מים

Electrochemical biosensor for rapid detection and quantification of Cyanobacteria toxins in water reservoirs

מוגש לקרן המדען הראשי במשרד החקלאות ופתוח הכפר ע"י:

דר' ספי ורניק, המכון להנדסה חקלאית, מנהל המחקר החקלאי-מרכז וולקני

דר' אור שפירא – המחלקה לאיכות ובטיחות ומזון, מנהל המחקר החקלאי, מרכז וולקני

Sefi Vernick, Department of Sensing, Information and Mechanization Engineering, Institute of Agricultural Engineering, ARO The Volcani Center, HaMaccabim Rd. 68; POB 15159, RishonLeZion 7528809, Israel

Orr Shapiro, Department of Food Sciences, Institute for Post-harvest and Food Sciences, AROThe Volcani Center, HaMaccabim Road 68, P.O.B 15159,RishonLeZion, Israel 7528809

תוכן עניינים

1. תקציר מדעי

א. הצגת הבעיה

הצטברותם של רעלנים המופרשים ע"י חיידקים כחוליים ובעיקר מיקרוציסטינים, במאגרי מים עיליים מהווה בעיה כלל עולמית. בעוד חשיפה לריכוזים גבוהים עלולה לגרום לתמותה וחשיפה כרונית תורמת להתפתחות סרטן, מדינות רבות בעולם אמצו תקן המתיר עד 1 מק"ג/ליטר של המיקרוציסטין MC-LR במי שתיה וצריכה יומית כוללת של לא יותר מ-0.04 מק"ג לק"ג משקל גוף. השיטות לזיהוי וכימות מיקרוציסטינים במים נשענות בעיקר על הפרדה כימית תוך שימוש במכשור יקר ומסורבל הדורש מיומנות וזמן הפעלה ממושך. בשנים האחרונות אומצו שיטות בעלות תפוקה גבוהה, ובעיקר כאלה המבוססות על מבחן אימונואנזימטי. על אף יתרונותיהן הרבים, שיטות אלו מצריכות כוח אדם מיומן ומעבדה ייעודית ועלותן עדיין גבוהה. לפיכך קיים צורך אמיתי ודחוף בפיתוח שיטות לזיהוי וכימות מהיר של מיקרוציסטינים "בנקודת הטיפול". במחקר זה אנו מבקשים לפתח התקן ביוסנסור אלקטרוכימי המבוסס על מערך של תאים אלקטרוכימיים ומכשיר מדידה המסוגלים להמיר את האות הביולוגי (קישור נוגדן או פעילות אניזמטית) לאות אלקטרוכימי (זרם נמדד). לצורך כך, במחקר זה ישולבו מספר גישות (מבוססות נוגדן – אימונואלקטרוכימיות וכן מבוססות אנזים הספציפי למיקרוציסטינים) עם שבב (ביוצ'יפ) המכיל תאים אלקטרוכימיים לצורך בניית ביוסנסור שיאפשר מדידה מדויקת ומהירה של מיקרוציסטינים בתנאי שטח.

ב. שיטות עבודה

מתודולוגיית העבודה במחקר זה מבוססת על יצירת תוצרים ביוכימיים, אלקטרוכימיים והנדסיים, אפיונם ושילובם לכדי ביוסנסור פונקציונלי. טיבו הבין תחומי של מחקר זה מכתיב שיטות עבודה מדיסציפלינות שונות. בחלקו הראשון של המחקר נדרשת עבודה מולקולרית ומיקרוביולוגית על מנת לאפיין ולכייל את ריכוז הנוגדן ויחס הנוגדן-אנטיגן (ELISA) ועל מנת להפיק את האנזים מיקרוציסטינז המבוטא בחיידקים. כמו כן, מאמצים ביוכימיים נדרשים על מנת להפריד את האנזים ולאפיינו וכן על מנת לבצע קישור כימי של נוגדן, אנטיגן ואנזים למיקרואלקטרודות. מדידות אלקטרוכימיות וולטמטריות ואמפרומטריות נדרשות על מנת לאפיין את התא האלקטרוכימי, ואת תלות הזרם הנמדד בריכוז הסמן האנזימטי. האספקט ההנדסי של המחקר כולל את תכנונם ועיצובם של הצ'יפים האלקטרוכימיים וכן את ייצורם בתהליכי פוטוליתוגרפיה, שיקוע פיסיקלי ואלקטרוכימי של שכבות דקות ואינטגרציה של האלקטרודות עם תא מדידה ייעודי.

ג. תוצאות עיקריות

לסיכום המחקר: בשנת המחקר הראשונה תכננו, פתחנו, ואפיינו שבב ביולוגי (ביוצ'יפ) המבוסס על מערך אלקטרוכימי ממוזער המיוצר בשיטות פבריקציה מיקרואלקטרוניות. כמו כן, פתחנו וייצרנו תא מדידה ייחודי המשלב את הביוצ'יפ, מתממשק למעגל מדידה חשמלי (פוטנציוסטט) ומאפשר הזרמת דוגמאות. במקביל, עלה בידנו להפיק את האנזים מיקרוציסטינז (MlrA) המבוטא ע"ג פלסמיד בחיידקי *E. Coli*,

לנקותו, ולבצע אפיון ביוכימי מקיף של האנזים. בשנת המחקר השנייה, פתחנו שיטת קיבוע של הנוגדן ע"ג האלקטרודות ואפיינו את הקיבוע. כמו כן, הדגמנו באמצעות הביוצ'יפ ותא המדידה שפיתחנו, עקומת כיול לטוקסין MC-LR עם סף רגישות חסר תקדים של 3 ננוגרם/ליטר, באמצעות מדידת עכבה אלקטרוכימית וכן חישת טוקסין במודל של מים מזוהמים בחיידקים. כמו כן, כחלק מהביוסנסור, פיתחנו אלקטרודה אנזימטית המכילה את האנזים MlrA בתווך של שכבת פולימר מוליך, והדגמנו כיצד בנוכחות הסובסטרט MC-LR, הפעילות הקטליטית של האנזים מותמרת לאות אלקטרוכימי הניתן למדידה בוולטמטריה פשוטה. בנוסף, יצרנו דגם משופר של פלטפורמת מדידה המאפשר מדידה סימולטנית של צ'יפים רבים תוך כדי הזרמת הדוגמאות. בשנה האחרונה פתחנו את שיטת ה-ECI - תבחין אימונו-אנזימטי אלקטרוכימי. אפיינו את מרבית הפרמטרים השונים המעורבים בתהליך והדגמנו מדידת זרם חשמלי הנובע מחיזור סובסטרט פעיל חשמלית כתוצאה מקישור טוקסין בתמיסה. הראינו שהאות הנמדד הינו ביחס הפוך לריכוז ה-MC-LR בדוגמה, כצפוי. בנוסף, המשכנו לשפר את שתי שיטות המדידה הנוספות. לבסוף, פרסמנו מאמר בעיתון מדעי מוביל בתחום, הצגנו חלק מעבודתנו במספר כנסים ורשמנו בקשה לפטנט.

ד. מסקנות והמלצות לגבי יישום התוצאות

1. תוצאות המחקר עוררו עניין רב בקרב מספר חברות תעשייתיות המתעניינות במדידת מזהמים במים וביניהן: חברת מקורות, חברת אטלנטיום, חברת BlueGreen ועוד.
2. על בסיס תוצאות המחקר זכינו במענק ("נופר") מרשות החדשנות ובתמיכת "מקורות" להמשך פיתוח הביוסנסור. מטרת המחקר הינה להתקדם בפיתוח בצורה משמעותית לכדי TRL 6-8
3. יש לציין כי ההתקדמות בשלש שיטות המדידה השונות שנכללו במחקר זה לא הייתה סימטרית. בעוד ששיטת EIS הניבה תוצאות מבטיחות כבר בשנה השנייה, מחקר רב הושקע בפיתוח שתי השיטות האחרות.
4. אנו סבורים כי נדרש מחקר המשכי על מנת להוכיח ניסיונית ובאמצעות מודל את השיפור בדיוק הדיאגנוסטי כתוצאה מבדיקה מקבילית ושילוב שיטות.

1. Introduction

Harmful blooms produced by Cyanobacteria (blue-green algae) are a worldwide problem in surface water and brackish water reservoirs[1]. This problem is well known in lakes undergoing eutrophication processes, including Lake Kinneret in drinking water reservoirs and effluent reservoirs. CB blooms can pose a significant health risk due to the production of toxins that are concentrated in water and can cause harm to humans and animals through drinking, swimming, and probably also eating food contaminated with the toxins[2,3]. These HCBs can contain multiple cyanotoxin (CT)-producing species. The toxins are collectively called cyanotoxins. Fish ponds are particularly prone to contamination, thus placing the aquaculture industry at risk[4]. Exposure to the toxins (e.g., Microcystins) is mainly associated with hepatotoxicity and carcinogenesis and leads to both acute and chronic damage[5,6]. Microcystin-LR (MC-LR), the most common microcystin, accounts for most of the reported poisonings and is considered an imminent threat to human and animal health. Consequently, stringent regulation has recently been imposed by the World Health Organization (WHO), limiting the allowed MC-LR concentration in drinking water to <1 µg/L and a maximal daily intake of 0.04 µg/kg body weight[7–9]. Current detection methods have proven relatively efficient in accurately quantifying MCs in water. However, conventional methods that are based on analytical and immunoassay techniques are time-consuming, demand highly skilled personnel and expensive equipment, and are not suited for on-site detection. Thus, there is an urgent need for an advanced portable detection tool to enable a frequent examination and quick monitoring of MCs in fish ponds, drinking water reservoirs, and other surface water. This would help mitigate the risks associated with the safety of aquaculture produce as well as drinking water and rapidly apply the necessary remedial measures. **The overall objective is to design and develop an electrochemical biosensing platform that can perform several complementary tests, combining immuno- and enzymatic (Fig. 1) assays for the detection of ultra-low concentrations of MC-LR in water, while increasing accuracy and reducing detection time**.

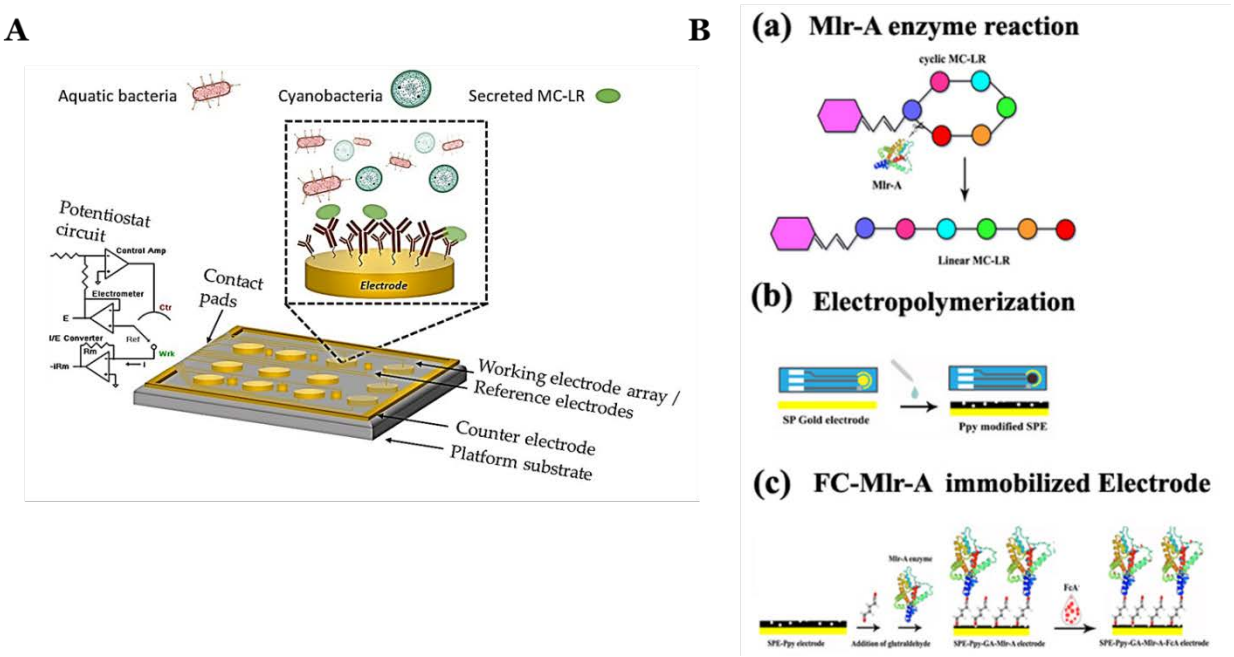

Fig. 1: Schematic illustration of the proposed biosensing system. A) A miniaturized array of electrochemical cells containing microelectrodes is produced by conventional microelectronics fabrication methods. After chemical modification of the surface of the electrodes, antibodies specific for the tested cyanotoxin are immobilized. The biochip easily connects to the "electronic reader", which is also portable (in a USB-stick form). Following exposure to a water sample that contains many organisms including cyanobacteria that secrete the target toxins, the toxins bind specifically to antibodies and thus result in a change in the electrical conductivity of the electrode. This change can be measured and processed in real time allowing the quantification of toxins in the sample. **B)** Schematic representation of Mlr-A enzymatic reaction (a), electro-polymerization of Polypyrrole (PPy) on a screen-printed gold electrode (b), and (c) covalent immobilization Mlr-A enzyme on PPy-modified SPE and Ferrocene functionalization.

2. Research objectives

This study seeks to develop an integrated multi-method biosensing system for rapid on-site detection of MC-LR. Immuno-electrochemical sensing employing anti-MC-LR antibodies and additional enzyme-based amperometry, employing the MC-LR degrading enzyme, MlrA, will be applied by a custom-designed biochip and a measurement platform. The electrochemical immunoassay (ECI) will enable highly sensitive detection of MC-LR via impedance spectroscopy and amperometry (using an equivalent ELISA method) while the enzyme-based electrode, comprising MlrA embedded in a conductive polymer, would complement the assay. Our specific objectives: ***i*)** create a fabrication process that would provide high quality electrochemical chips containing micro-electrodes, with a very high yield, ***ii*)** develop and fully characterize electrode bio-functionalization methods that include the conjugation of antibodies, antigens, and enzymes, ***iii*)** demonstrate the feasibility of the biosensor to detect different

concentrations of MC-LR while exceeding the reported limit of detection, ***iv*)** develop the biosensor measurement platform that comprises the biochip, the electrical contacts, and the liquid chambers, ***v*)** demonstrate the combined electrochemical detection of MC-LR by applying different methods with the same biochip platform.

3. Main Results

3.1. Electrochemical chip fabrication: biochips were designed as electrochemical cells with a three-electrode configuration (working, counter and reference electrodes), microfabricated on a p-doped Si/SiO_2 substrate (with 285 nm thermally grown oxide) by a combination of photolithography (to define the electrodes pattern) and sputtering (gold deposition). The process flow showing the step-by-step fabrication of electrochemical chips is shown in Fig. 2. The wafer-scale fabrication yielded 31 chips, each comprising three gold electrodes (100 nm thick Au layer) as well as contact pads. The working electrode diameter was 0.6 mm. On-chip Ag/AgCl reference electrodes were prepared in-house by electroplating and the individual chips were finally diced. The generated chips were characterized electrochemically and by scanning electron microscopy.

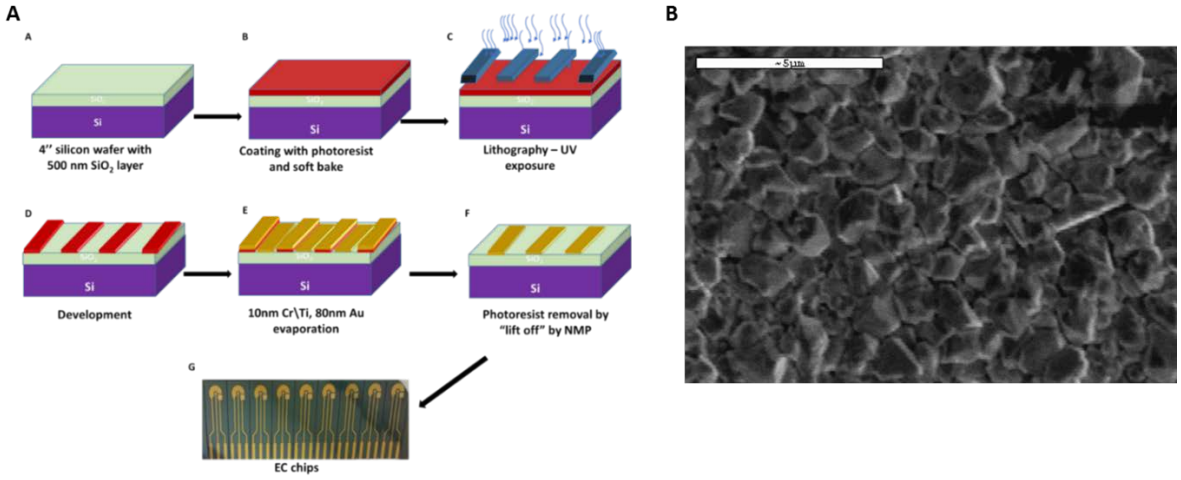

Fig. 2. Fabrication of electrochemical chips. **A**. process flow of chip fabrication by photolithography and sputtering: (a) The wafer is cleaned with acetone, isopropanol, and distilled water; (b) Photoresist (PR) coat is spun onto the wafer and soft baked. C) Patterns are projected onto the wafer (photolithography); D) The substrate is developed and unexposed PR is removed. E) Titanium and gold are sputtered onto the substrate F) The PR and gold are removed by a lift-off process. Following this, the wafer is rinsed with ACT, IPA, and DI, and G) The wafer is ready for electroplating. **B**. Following fabrication (and surface characterization of the deposited electrodes), the reference electrodes are electroplated. Briefly, the formation of a reference electrode is carried out by electroplating silver (from a silver plating bath) followed by anodic generation of a silver chloride layer to obtain a silver/silver chloride

layer (Ag/AgCl). The electroplating of silver yields a typical white luster deposit that appears, in a SEM analysis, as a homogenous crystalline deposit with dense Ag nuclei of ~1µm (Bar: 5 µm).

3.2. Electrochemical Characterization of chips: The quality of the electroplated Ag/AgCl quasi reference electrode (RE) and of the whole cell were electrochemically characterized. The RE potential demonstrated a linear dependence on the electrolyte (NaCl) concentration log, as expected, following the Nernst equation (Fig. 3).

An example of cyclic voltammetry (CV) for the EC biochip is presented in Fig. 4A, where four different scan rates were used consecutively. The peak heights increased with increasing scan rates and were linearly proportional to the square root of the scan rates (Fig. 4B), as expected, following the Randles-Sevick equation. In addition, the peak separation was not significantly affected by the scan rate (Fig. 4C).

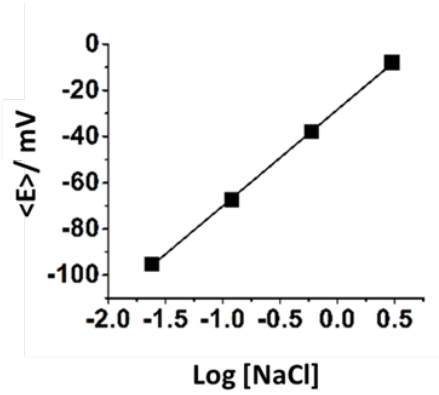

Figure 3. Characterization of the RE. Verification of a newly formed Ag/AgCl reference electrode is carried out by measuring its potential versus a commercial reference electrode in varying electrolyte (KCl) concentrations. The response of the electrode is plotted against the log[KCl] such that any log change in KCl concentration is expected to yield a 59 mV potential difference, according to the Nernst equation. In practice, deviations from this value are expected to evolve from the nature of the measured electrode (an open reference electrode), the quality differences, and experimental conditions (mainly varying distances between the measuring electrodes that affect solution resistance). Our reference electrodes demonstrate a 'Nernstian behavior', close to the theoretical value.

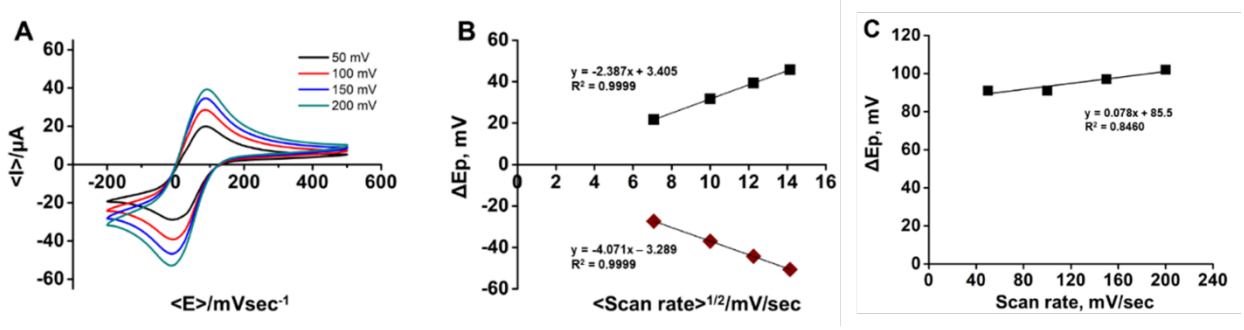

Figure 4. Characterization of the EC cell. Verification of the whole cell is obtained by i-E curve (cyclic voltammogram) with the well-known redox couple ferricyanide. **A**. CV at different scan rates with a solution of 20Mm ferricyanide/ferrocyanide. Four different scan rates were used, consecutively. **B**. Corresponding analysis obtained from the biochip. The peak height increased as the scan rate increased and was linearly proportional to the square root of the scan rate, showing the anodic peaks (top) and cathodic (bottom). C) peak separation is relatively independent of scan rate.

3.3. Development of biochip and an electrochemical (EC) biosensing platform.

An in-house Polytetrafluoroethylene (PTFE) apparatus providing electrical contacts for EC chips and serving as a platform that enables simultaneous measurement of multiple chips and continuous flow was developed (Fig. 5). The purpose of the platform is to integrate all the components of the EC biosensing platform, including a flow channel, biochips, and contacts, and to easily interface with a commercial potentiostat and to enable simultaneous measurement of multiple chips.

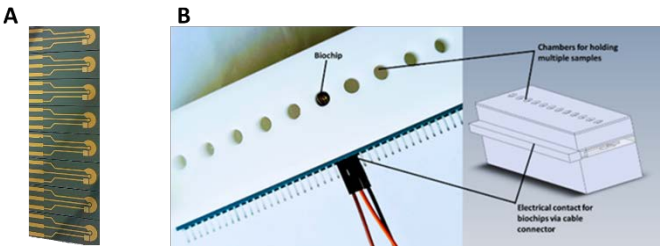

Fig. 5. The biosensing platform. A. Silicon-based electrochemical chips are microfabricated using photolithography and metal deposition. **B.** Custom manufactured apparatus. Image of a machined PTFE apparatus providing electrical contacts to electrochemical chips and chambers for interrogating multiple samples.

3.4 Electrochemical impedance spectroscopy (EIS): Impedimetric immunosensors are based on immobilized antibodies to detect antigens using EIS on a solid-state electrode. This detection method is based on the direct detection of antibody-antigen via binding of a target analyte to a biofunctionalized chip (biochip). Impedimetric immunosensors show great promise in rapidly detecting low concentrations of target antigens within a highly simplified testing setup. We sought to demonstrate this diagnostic potential by developing a miniature electrochemical biochip, integrating it with a monoclonal antibody (mAb) targeted against the microcystin MC-LR, and applying the developed immunosensor in the rapid detection of low MC-LR concentrations. A schematic illustration of the developed biochip and method is presented in Fig. 6A.

3.4.1 *Electrochemical measurements:* The EIS method measures the current response to an AC voltage over a frequency range. In a faradaic impedance measurement, a small sinusoidal AC voltage probe is applied while monitoring the current response at different frequencies. The real (resistive) component of the impedance (determined by the in-phase current response) is plotted against the imaginary (capacitive) component (determined by the out-of-phase current response) to frequency. Both are described by $Z' = R_s + \frac{R_{ct}}{1+\omega^2 R_{ct}^2 C_{dl}^2}$ and $Z'' = \frac{R_{ct}^2 C_{dl}\omega}{1+\omega^2 R_{ct}^2 C_{dl}^2}$, where R_s is the solution resistance, R_{ct} is the

charge transfer resistance, C_{dl} is the double-layer capacitance, and ω the angular frequency, which is commonly represented in a Nyquist plot (Fig. 6B). The Nyquist plots arising from EIS measurements were fitted to the following Randles circuit from which the parameter of interest, R_{ct}, values were calculated: If an analyte affects one of these circuit parameters, then impedance methods can be used for analyte detection. The R_{ct} depicts the opposition experienced to electron movement and it increases in the presence of bound biomolecules. For a one-electron process, the R_{ct}, which controls the electron transfer kinetics of $Fe(CN)_6^{4-/3-}$ at the interface of the electrode, can be described by: $R_{ct} = \frac{RT}{F^2\kappa^2 C}$ where R denotes the gas constant, T is temperature, F is Faraday constant, κ^0 is the electron transfer rate constant, and C is the concentration of the electroactive species[11,12]. The semi-circular region represents a slower charge transfer at higher

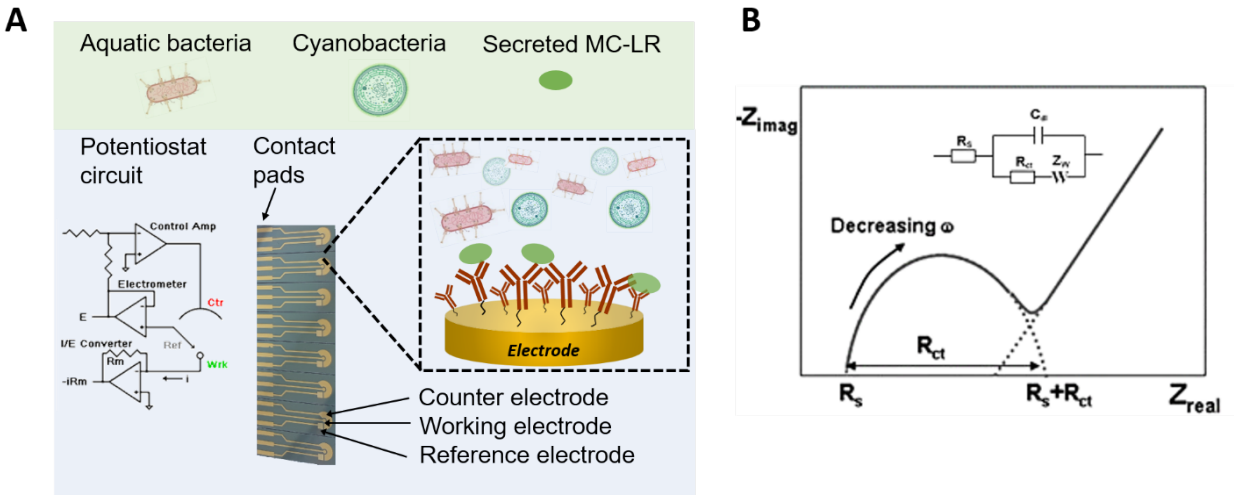

Fig. 6. EIS-based biosensor for MC-LR detection. A. Schematic illustration of the developed biochip. Multiple electrochemical cells are fabricated by microelectronic manufacturing techniques. Anti-MC-LR monoclonal antibodies are chemically modified and covalently immobilized to an activated gold working electrode surface. The biochip is interfaced with a portable potentiostat device (a generalized circuit diagram is shown on the left). Exposure to a water sample contaminated with MC-LR-secreting cyanobacteria results in specific binding of the toxins to the electrode-bound antibodies, affecting the electrode's impedance. This change can be measured and analyzed in real-time, allowing the quantification of toxins in the sample. **B.** An EIS measurement is used to interrogate the electrochemical system and separate the individual components that affect the circuit. A Nyquist plot depicts the change in the "real" component of the impedance (Z' or Z_{real}) versus the "imaginary" component (Z'' or $-Z_{imag}$, which results from capacitance) over a wide range of frequencies. The generated Nyquist plot is fitted to an equivalent circuit from which the different resistance values are extracted (inset). Solution resistance, R_s, charge transfer resistance, R_{ct}, Warburg resistance, Z_w, and double layer capacitance, C_{dl}, can all be modeled and calculated. Adapted from ref. ([18])

frequencies, whereas the straight line describes a faster mass transfer at lower frequencies. Also, a change in Warburg impedance, Z_w, dominated by mass transfer, can

occur when the diffusional transport of electroactive species from the bulk solution to the electrode surface is impeded due to the binding of biomolecules and targets onto the electrode[13]. However, both R_{ct} and Z_w depend on the concentration of electroactive species and the applied potential[14].

3.4.2 *Modification of EC chips with antibodies:* The immobilization strategy of antibodies is of critical significance in the development because it determines the orientation of the antibody on the electrode's surface. Our immobilization approach is based on the direct covalent attachment of thiolated antibodies to an activated gold electrode surface. The gold surface of the working electrode (WE) can be readily reacted with the sulfur head of thiolated molecules (following activation to yield the desired functional groups for subsequent immobilization). An anti-MC-LR Mab was thiolated using Traut's reagent (2-IT) via thiol-activation of primary amines (-NH_2) of the Mab, following the mechanism shown in Fig. 7A. The introduced sulfhydryl (–SH) group provides a strong affinity to a gold surface, thus enabling the covalent immobilization of the antibody. The thiolation reaction was optimized to obtain an average of ~6 –SH group per antibody by tuning the ratio of reagent to antibody. This fine-tuning enables control of the level of thiolation.

The estimation of introduced sulfhydryl groups was performed by Ellman assay used to quantify the number or concentration of thiol groups in a sample. Ellman's reagent (5,5′-dithiobis-(2-nitrobenzoic acid, or DTNB) quantifies the number or concentration of thiol groups in a sample. It is very useful as a sulfhydryl assay reagent because of its specificity for -SH groups at neutral pH, high molar extinction coefficient, and short reaction time. DTNB reacts with a free sulfhydryl group to yield a mixed disulfide and 2-nitro-5-thiobenzoic acid (TNB). The target of DTNB in this reaction is the conjugate base (R—S-) of a free sulfhydryl group. TNB is the "colored" species produced in this reaction and has a high molar extinction coefficient with a value of 14,150$M^{-1}cm^{-1}$ at 412nm. The DTNB reduction reaction and its structure are shown in Fig 7B. Introduced –SH groups were quantified by reference to the extinction coefficient of TNB following: $C=A/bE$; where A=absorbance, b=optical path length (cm), E=molar extinction coefficient, and C= concentration (molar).

Antibodies incubated with Traut's reagent at a ratio of 1:10 and 1:15 yielded an average -SH groups per antibody of 3.63 and 6.7, respectively.

Gold surfaces can be readily reacted with the sulfur head of thiolated molecules enabling the immobilization of biorecognition molecules[10]. An assessment of the immobilization efficiency was carried out by fluorescence microscopy analysis, using a fluorescently (Cy3)-labeled thiolated antibody compared with a non-thiolated antibody. Fluorescence microscopy images shown in Fig. 7C confirm the immobilization of antibodies to the gold electrode. Electrode surface characterization by AFM, as shown in Fig. 7D, provides further indication for the immobilization of antibodies.

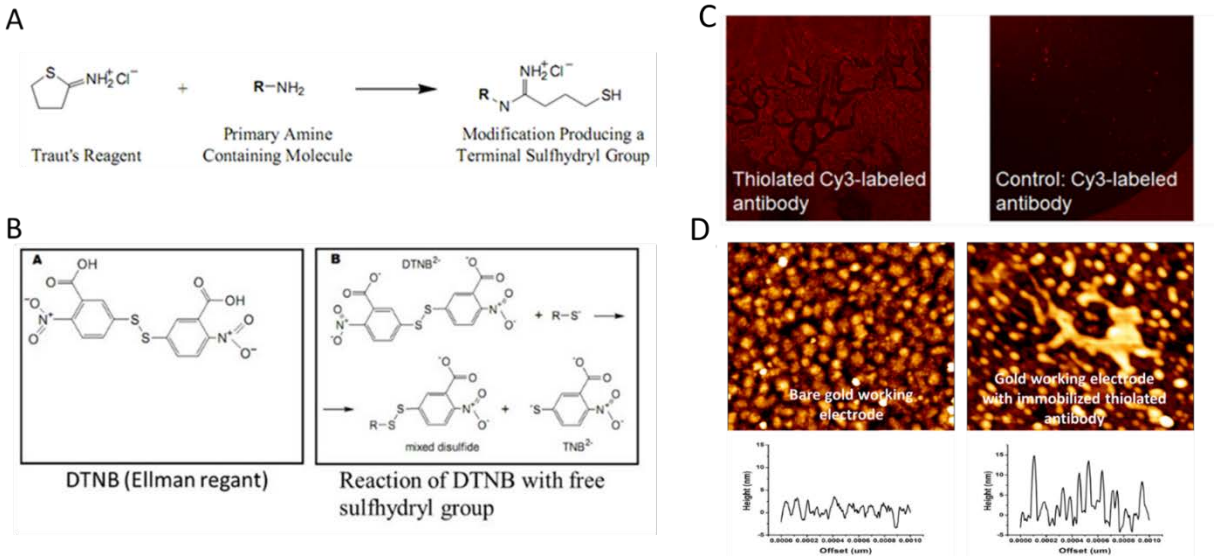

Fig. 7. Biofunctionalization of EC chips. **A**. Immobilization of antibodies is based on covalent attachment using well-established gold-thiol chemistry. Antibodies were thiolated by using the thiolating reagent 2-imminothiolane hydrochloride (Traut's reagent), which reacts with primary amines (-NH_2) to introduce sulfhydryl (-SH) groups while maintaining charge properties similar to the original amino group. The reaction was optimized to obtain an average of ~6 –SH group per antibody. **B.** Ellman assay using DTNB (left) was used to assess the thiolation efficiency. The reaction is monitored by a spectrophotometer. **Surface characterization of functionalized electrodes: C.** Assessment of thiolated antibodies immobilization to the gold working electrode is carried out by fluorescence microscopy analysis. Thiolated Cy3-labeled antibody is incubated on the gold WE. As a control, a non-thiolated Cy3 antibody was used. Incubation is followed by rigorous rinsing of the electrodes. **D**. AFM image of gold working electrode surface before and after the covalent immobilization of thiol-modified antibodies.

This direct approach to electrode functionalization is advantageous compared to well-established self-assembled monolayer (SAM) generation methods since it involves a straightforward preparation and avoids complete electrode passivation often attained with SAM. Furthermore, this functionalization procedure can be readily scaled up, as it is compatible with microarray printing technology.

To measure the effect of immobilized antibodies on the R_{ct}, impedance spectra were recorded and analyzed before and after antibody immobilization, and these were compared with measurements taken after 30 minutes of incubation with MC-LR, as shown in Fig. 9. It should be noted, that a 10 min incubation was found to significantly affect the recorded impedimetric signal, as shown in Fig. 8. Using the Nyquist plots, we observed the effect of antibody immobilization on the R_{ct}. In a bare electrode, the R_{ct} is small and impedance is dominated by the diffusion of the electroactive species, the so-called Warburg impedance, which is evident in low frequencies. Following antibody immobilization, the Warburg impedance is no longer a significant factor. Instead, the contribution of R_{ct} to the impedance becomes largely dominant as an insulating layer of biomolecules is attached to the surface. Incubation with a solution containing 3 µg/L MC-LR resulted in a further increase in R_{ct}, as the bound toxin further ads to the resistive component of the impedance.

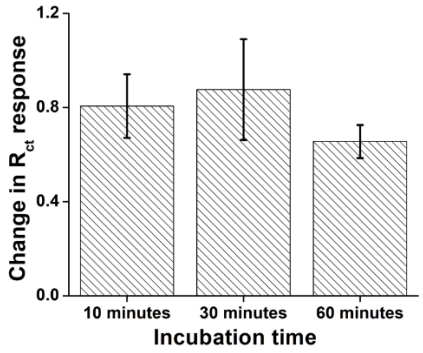

Fig. 8. Nyquist plots of antibody-functionalized electrodes following incubation with MC-LR. Change in R_{ct} signal following MC-LR binding to MC10E7/GE at different incubations times was evaluated. Measurements conducted in PBS pH 7.4 containing 10 mM $Fe(CN)_6^{4-/3-}$ and 0.1 M KCl show the dependence of impedimetric response (R_{ct}) on immunoreaction time. Bar plots (change in R_{ct} response) were calculated from the ratio of MC-LR/MC10E7/GE and MC10E7/GE normalized to 1 (error bars: SEM, n=3).

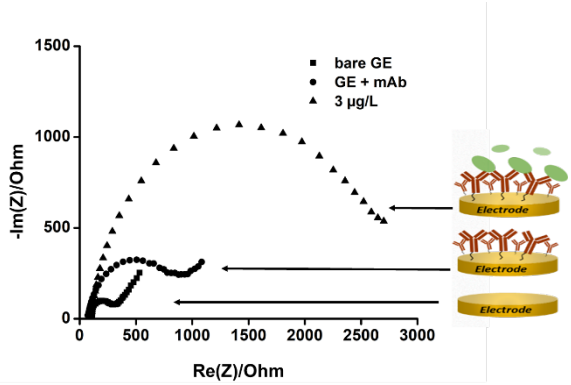

Fig. 9. EIS response of the developed immunosensor. The impedance spectra of a bare electrode ('bare GE') are characterized by low charge transfer resistance (R_{ct}) and high Warburg (Z_w) impedance. After antibody immobilization ('GE+mAb'), the R_{ct} increases, and the Z_w is no longer dominant. Following the binding of the toxins ('3 µg/L'), the R_{ct} increases dramatically. This increase is proportional to the concentration of the bound toxin and allows its quantification in the sample.

The sensitivity and dynamic range of the device were measured by briefly immersing biochips in MC-LR solutions with concentrations spanning six orders of magnitude, from 0.0003 µg/L to 30 µg/L, as shown in the Nyquist plots of Fig. 10A. The addition of MC-LR was found to affect R_{ct} in a dose-dependent manner, clearly seen in Fig 10B, with a positive correlation observed between MC-LR concentration and R_{ct} response. The calibration curve of the R_{ct} response exhibited an exponential dependence ($R^2 = 0.9812$) (Fig. 10C). Nonlinear calibration curves have been previously reported in impedimetric biosensors[15,16]. The inset in Fig. 10C shows a linear response ($R^2 = 0.9915$) to the log of MC-LR concentrations ranging between 0.003 µg/L to 3 µg/L, with 0.003 µg/L yielding a mean R_{ct} increase of 40.8 %(±3.4) while 3 µg/L affected a mean R_{ct} increase of 143.3 % (±10.1).

The applicability of the immunosensor was further demonstrated by detecting MC-LR in bacterial suspensions of *Microcystis aeruginosa PPC 7806* and *Spirulina sp.,* used as models for contaminated water. These samples represent highly complex matrices containing various aquatic bacteria, biomolecules and cell debris, as evident by the images shown in the inset of Fig. 10D. Both raw and filtered *Microcystis aeruginosa PPC 7806* samples (2.08×10^7 cells/mL) demonstrated an increased impedimetric response, as shown in Fig 10D. Higher R_{ct} values were consistently recorded for filtered samples (mean R_{ct} change = 1.33 ± 0.77), compared to unfiltered samples (mean R_{ct} change = 0.85 ± 0.46), both relative to the antibody-modified electrode. Incubation with the non-CT-producing *Spirulina* suspension (4.9×10^7 cells/mL), used as a negative control, did not affect the recorded impedance, as shown in Fig. 10D. In addition, no response was observed when MC-LR was incubated on electrodes functionalized with a non-specific antibody, mAb-EspB-B7 (that targets the virulent EspB protein in pathogenic *E. coli* [17]). The Nyquist plots of these control measurements clearly demonstrate the specificity towards MC-LR, lending further support to the feasibility of our detection method.

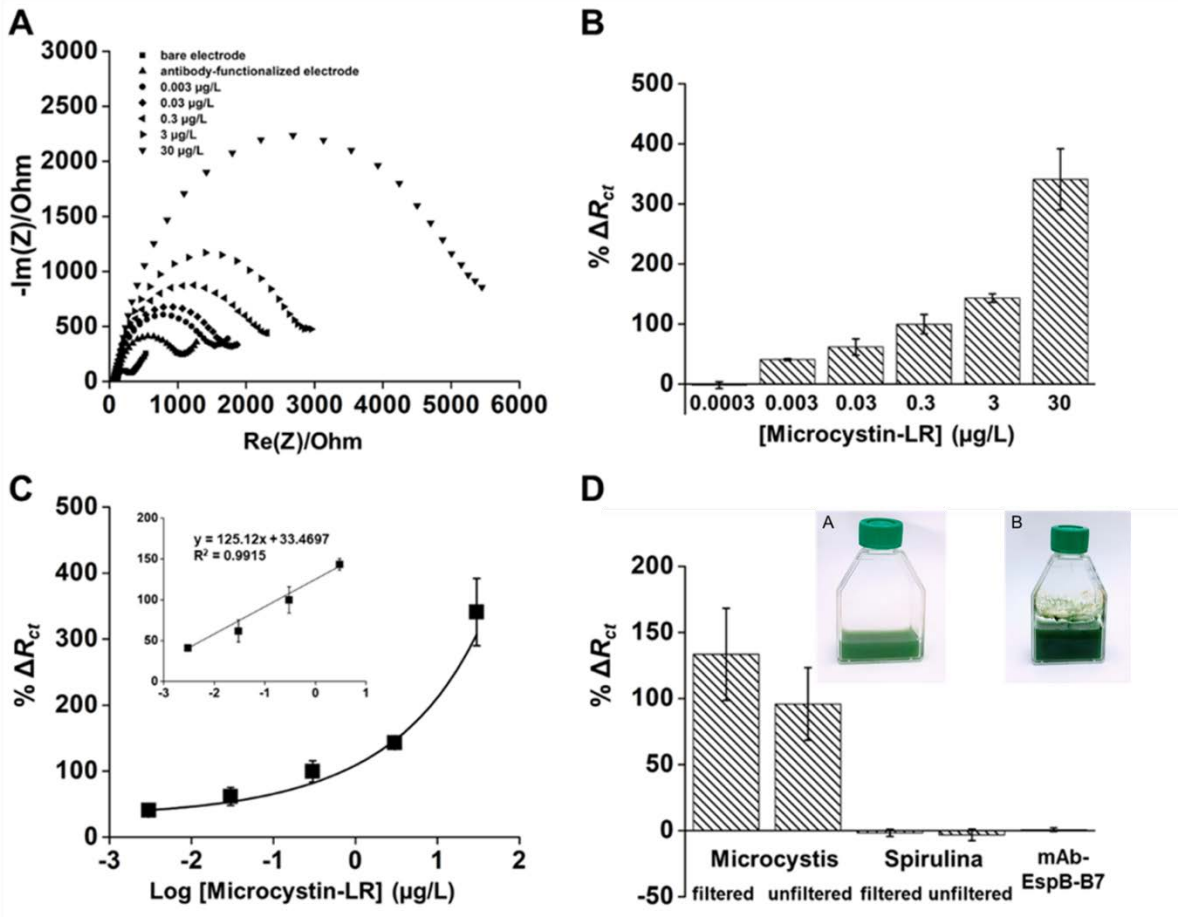

Fig. 10. MC-LR detection with an impedimetric immunosensor. A. The obtained Nyquist plots from measurements of a bare gold electrode ('bare GE'), electrode after the immobilization of anti-MC-LR mAb ('GE + mAb'), and after incubating with six different concentrations of purified MC-LR toxin: 0.0003, 0.003, 0.03, 0.3, 3, and 30 µg/L. (The lowest concentration yielded a similar impedimetric signal as the background). **B.** Relative R_{ct} values of purified MC-LR toxin protein demonstrating a dose-dependent increase in R_{ct}. **C.** An exponential increase in R_{ct} is observed. Inset shows a linear dependence at lower concentrations, yielding a calibration curve for target MC-LR. **D.** Detection of MC-LR from cyanobacterial suspensions is feasible with the developed biosensor. Specific binding of MC-LR, contributing to an increase in R_{ct} is indicated with Microcystis suspensions, whereas no response was observed with Spirulina suspensions. Higher signals were obtained from filtered Microcystis suspension, as expected. Incubation of MC-LR on an electrode functionalized with an unrelated antibody (mAb-EspB-B7), showed no MC-LR binding, further supporting the specificity of the biosensor. The changes in R_{ct} values ($\%\Delta R_{ct}$) are the means of the R_{ct} ratios (before and after antigen-capture), calculated from triplicates. The error bars represent ± SD. **Inset of Fig D: Raw cyanobacterial cultures used as a model for contaminated water.** bacterial cell suspensions of: **A.** Microcystis aeruginosa PPC 7806 and, **B.** Spirulina sp. Both samples were cultured, grown, and maintained in BG-11 at a temperature of 24-26^{o}C and light intensity of 6 µmol photons m^{-2} s^{-1}**.**

3.5 Electrochemical Immunoassay (ECI). A second detection method is an EC indirect competitive Enzyme-linked immunosorbent assay (*ic*-ELISA). It is based on substrate-mediated amperometric detection of MC-LR, whereby the level of surface-

bound enzyme immunoconjugate following catalysis of an electroactive substrate is evaluated by a chronoamperometric detection using various standard MC-LR concentrations and raw cyanobacteria culture samples. A schematic description of the method is shown in Fig. 11.

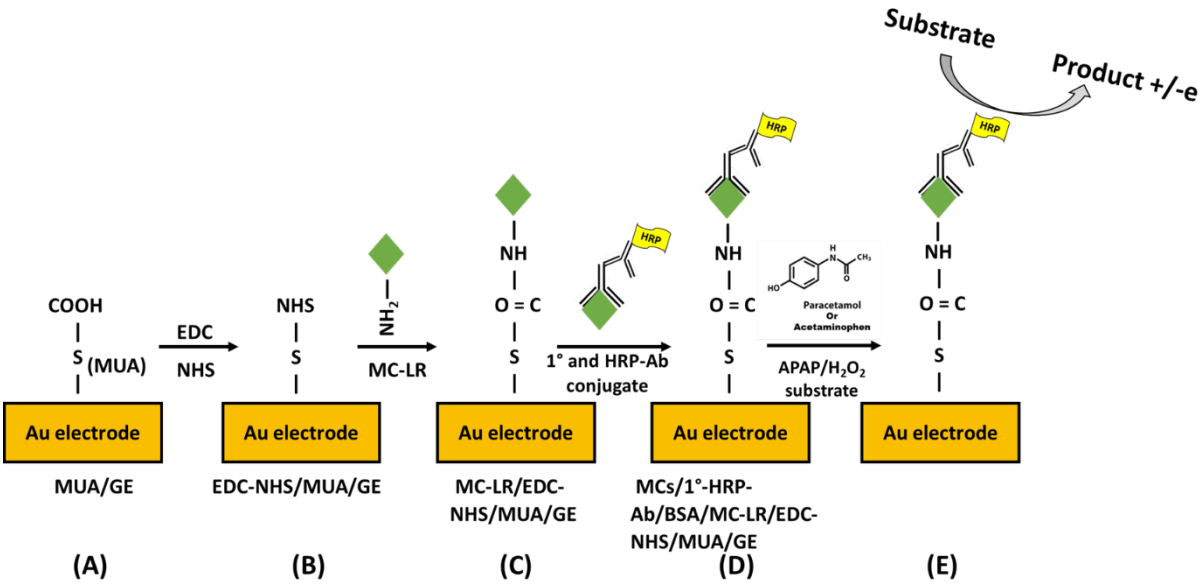

Fig. 11. Schematic description of the steps involved in the development of the amperometric biosensor for the ECI assay.

This chronoamperometry uses a fixed potential and measures the reduction current of an electroactive substrate as a function of time.

We first developed a conventional ELISA using a chromogenic reagent and obtained an MC-LR detection limit of 0.03 µg/L (Fig. 12A) and a linear fit of quantitative detection ranging from 0.1 µg/L to 3 µg/L (Fig. 12A). Then, we have characterized the electroactive substrates and enzyme (Fig. 12B) and the MC-LR toxin (Fig. 12C). As previously mentioned, the substrate APAP (Acetaminophen) is oxidized by the immuno-conjugate enzyme, horse-radish peroxidase (HRP), into the electroactive product NAPQI. The irreversible electro-reduction of NAPQI was measured at a potential of -100 mV. This potential was applied in the ECI to monitor the reduction of NAPQI following incubation with samples containing different concentrations of MC-LR and after incubation with the primary antibody and secondary antibody-enzyme complex, as shown in Fig. 13. The current signal resulting from the binding of the secondary antibodies to the coated

electrodes was inversely proportional to the concentration of MC-LR in the samples, as expected. At a high concentration of 1.65 µg/ml (mg/L) the current signal ratio (relative to background) was =1.5 whereas lower concentrations exhibited higher currents signal ratios (2.3 for 0.33 µg/ml and 8 for 0.066 µg/ml).

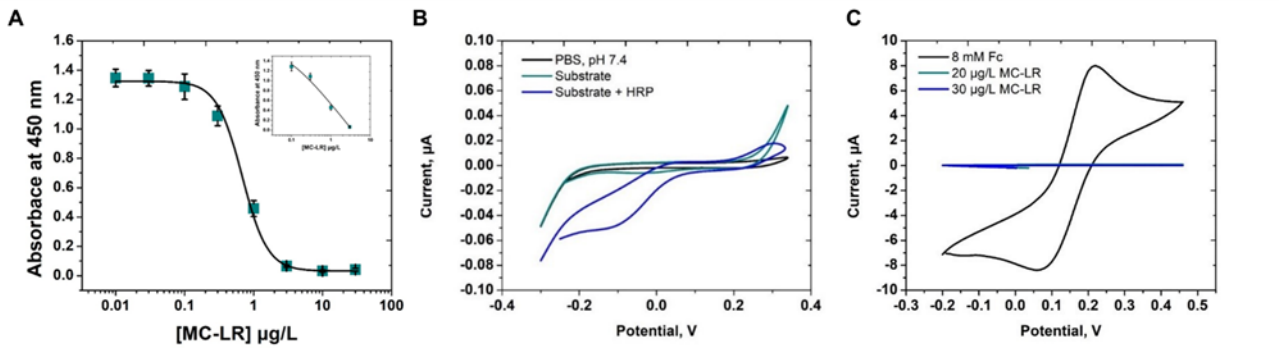

Fig. 12: Development of ECI based on ic-ELISA. A) A standard curve of ic-ELISA for MC-LR at concentrations ranging from 0.03 µg/L to 30 µg/L (error bars: SD, n=8). It was measured in eight repeats. ELISA plate wells were coated with 3 µg/mL MC-LR toxin. The antibody MC10E7 dilution was 1:3,000; enzyme Immunoconjugate dilution was 1:4,000. The experimental data are shown as discrete plot with error bars in black. The solid black curve fits the Hill equation to the experimental data and the inset image is the range of quantitative detection with good linearity. **B)** Cyclic voltammetry at a scan rate of 50 mV/sec of PBS, pH 7.4 with the substrate (a mixture of 0.3 mM H_2O_2, and 0.45 mM APAP), and the reaction of HRP with the substrate. Scan initiated following 1min incubation of solution reactants. CVs were performed separately. **C)** Cyclic voltammograms of 8 mM $Fe(CN)_6^{4-/3-}$ and two different concentrations of MC-LR solutions (20 and 30 µg/L) in PBS (pH 7.4) at a scan rate of 100 mV/sec.

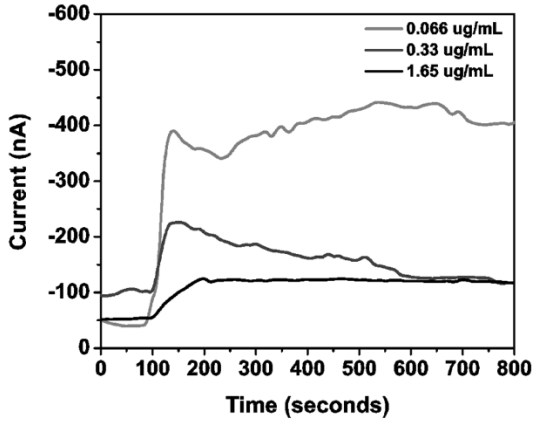

Fig. 13. ECI for the detection of MC-LR. The assay is designed as an EC equivalent of indirect competitive ELISA where the biochip electrode surface is coated with MC-LR and incubated with the primary (anti-MC-LR) antibody followed by a secondary antibody-HRP enzyme complex. Subsequent incubation with a sample containing a high MC-LR concentration affects the release of surface-bound antibodies due to competition and the decrease of the redox current. In contrast, low concentration of sample MC-LR results in a high redox current.

3.6 Development of Microcystinase (MlrA)-based electrochemical system for MC-LR detection.

3.6.1 *Expression and Purification of MlrA.* The heterologous expression of MlrA with his-tag in *E. coli* (BL 21) host, using pET21a expression vector was performed. The expressed MlrA was isolated, quantified (4.0 mg/mL of proteins), and characterized by an MlrA assay. The initial velocity of MlrA (V_0) was calculated (0.05 µM/min) and it was found that 50% of cyclic MC-LR hydrolysis was achieved within 13-15 mins (Fig. 14A). The maximum velocity of the MlrA enzyme was also calculated using the Hill equation and plot. The kinetic parameters V_{max}=9.53 µM/min, $K_{0.5}$=4.77 µM, and n=1.40 were obtained from the plot (Fig. 14B). Hill coefficient (n) greater than 1 indicates a positive co-operativity between substrate MC-LR and MlrA enzyme.

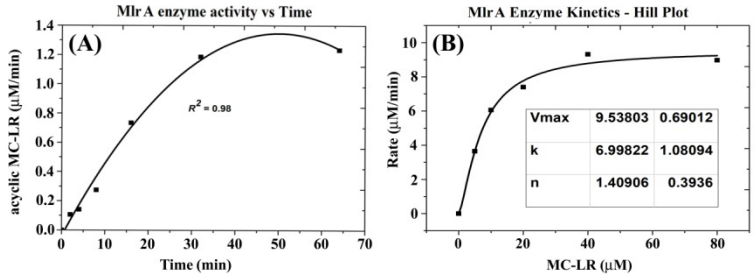

Figure 14: MlrA enzyme kinetics study. A) Determinination of iInitial velocity of MlrA enzyme and MlrA enzyme kinetics – Hill Plot (B).

3.6.2 *Electrochemical study of MC-LR and MlrA enzyme using unmodified SPE (screen-printed electrodes).* First, MC-LR and MlrA were studied electrochemically and found to have no electroactivity under the applied potential window. However, MC-LR was shown to significantly affect the non-faradic (charging) current, as opposed to MlrA. As seen in Fig. 15A (black bar), following MC-LR addition, the charging current increases dramatically, by up to 95%, and remains relatively stable over time (up to 30 mins). The charging current is likely attributed to the adsorption of MC-LR to the electrode surface. The slight decrease in the charging current following 20 min incubation suggests a desorption mechanism that is time and voltage-dependent.

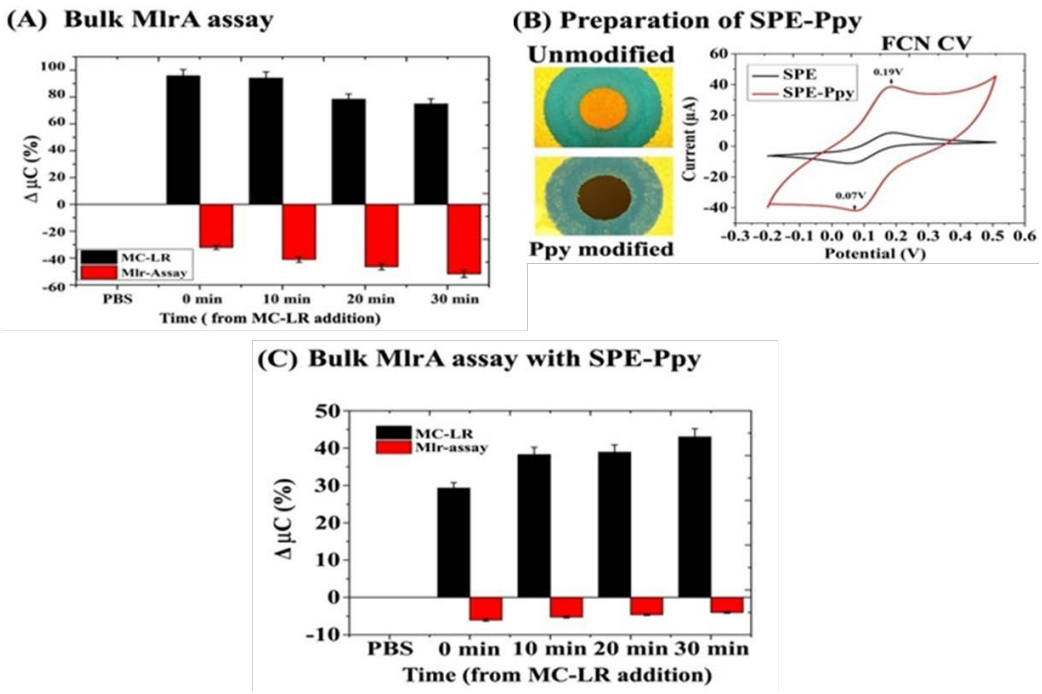

Fig. 15: Electrochemical analysis of MlrA assay with cyclic MC-LR using unmodified SPE A). Black and red bar graphs indicate the capacitance of MC-LR and MlrA assay, respectively, at different incubation times. B). Polypyrrole modified working electrode and their corresponding FCN CV with control. C) Electrochemical analysis of MlrA assay with SPE-Ppy. Black and red bar graphs indicate the capacitance of MC-LR and MlrA assay, respectively, at different incubation times. Error bars show standard deviations of means for triplicate ($p = < 0.05$).

The effect of MC-LR enzymatic degradation was also studied. The addition of MC-LR to a MlrA-containing solution results in a gradual decrease in charging current over time (Fig. 15A, red bar). A decrease of 32% was observed following MC-LR addition, further decreasing by 52% after 30 min incubation. The addition of MlrA alleviated the capacitive effect observed during the CV measurement of MC-LR. These findings suggest that the binding of MlrA to MC-LR may hinder its adsorption to the electrode surface. The gradual decrease in capacitance may also indicate that the linearization of the cyclic MC-LR, catalyzed by MlrA, yields a less adsorptive product. Seemingly, the hydrolysis reaction did not involve any redox activity or charge transfer [19]**.**

However, to better associate MlrA reaction with charge transfer, an *enzyme electrode* needs to be constructed. To facilitate effective wiring of the MlrA active site to the electrode surface, a conductive polypyrrole (Ppy) layer was electro-polymerized on the working electrode, as seen in Fig.15b (left). Ppy-modified SPE (SPE-Ppy) was characterized by CV using the Ferrocyanide (FCN) redox couple. The anodic and

cathodic currents increased significantly up to ~ 6 ± 0.2 times higher than unmodified SPE, as shown in Fig. 15B (right). The SPE-Ppy electrode was then used to study the MlrA assay electrochemically in bulk solution. A CV analysis revealed an increase in the charging current following the addition of MC-LR, similar to that measured with the unmodified SPE. Current levels remained relatively stable over time, as shown in Fig. 15C (black bars). Upon the addition of MlrA, a significant decrease in charging current was observed, in a similar fashion to that obtained with an unmodified SPE, as shown in Fig. 15C (red bars). Although current amplitudes were, as expected, significantly higher in the case of SPE-Ppy compared with unmodified SPE, the relative change was significantly lower. As seen in Fig. 15C, the addition of MC-LR to SPE-Ppy resulted in a 29% increase in charging current, compared with an 80% increase previously measured with an unmodified SPE. Accordingly, the addition of MlrA has decreased the charging current by 4%-6% with the SPE-Ppy compared to a decrease of 30%- 50% measured with unmodified SPE. These findings indicate serial capacitance following MC-LR adsorption.

Monitoring the charging current may therefore serve as an indicator of the enzymatic breakdown of cyclic MC-LR in real-time and provide useful information. In the next step, MlrA enzymes were covalently immobilized to the SPE-Ppy surface via a glutaraldehyde cross-linker (Fig. 1B-c).

3.6.3 *Covalent Immobilization of MlrA enzyme on SPE-Ppy using glutaraldehyde crosslinkers.* Fig. 16A illustrates the FCN CV for unmodified SPE, Ppy-modified SPE, and MlrA covalently immobilized to SPE-Ppy electrodes. The immobilization of MlrA was clearly indicated by the reduction in redox peaks.

A redox mediator is often included to enable EC detection when using enzymes that lack a measurable redox activity. Consequently, we conjugated a ferrocene molecule (Ferrocene carboxylic acid, FcA) to MlrA. The yield of FcA conjugation, estimated from CV data, was found to be 4.3-6% and the calculated number of FcA molecules per MlrA was found to be ~7. Furthermore, the residual enzymatic activity of MlrA-FcA bioconjugates was investigated by MlrA assay and HPLC analysis, and found to be lower by a factor of 3.5 compared to the unmodified enzyme due to the functionalization (Fig.

16B). MlrA-FcA conjugates were used for the preparation of SPE-PPy-GA-MlrA-FcA electrode.

3.6.4 *Electrochemical detection of MC-LR using enzyme electrodes.* The SPE-Ppy-GA-MlrA electrodes were used to monitor the MlrA assay by measuring charging currents during a 30 min period (Fig. 16C). In these recordings, a gradual increase in charging currents (from 26% to 53%) was observed over time following MC-LR addition. These results suggest that despite the proximity of the enzyme to the electrode surface, an effective catalysis-related charge transfer does not occur. Alternatively, the residual activity of MlrA may be dramatically affected. Such charge transfer may be facilitated by employing a redox mediator, as previously described. Therefore, a similar experiment was carried out using a MlrA-FcA conjugate, covalently immobilized to SPE-Ppy electrode via GA cross-linker. Indeed, a gradual decrease in charging current (from -8% to -23.3%) was observed over 30 min following MC-LR addition (Fig. 16C, red bar). These findings significantly differ from the results obtained without the redox mediator, suggesting that the EC wiring of MlrA can only be achieved by using an electroactive mediator and that conjugation of such mediator may effectively "restore" the residual enzymatic activity that was reduced due to immobilization and bioconjugation. Overall, the MlrA-immobilized SPE-PPy electrodes may be used to monitor the enzymatic cleavage of MC-LR in real-time.

Furthermore, combining these enzyme electrodes with electro-immunoassay on a single platform may serve as an ideal tool for monitoring and detecting cyanotoxins with high specificity.

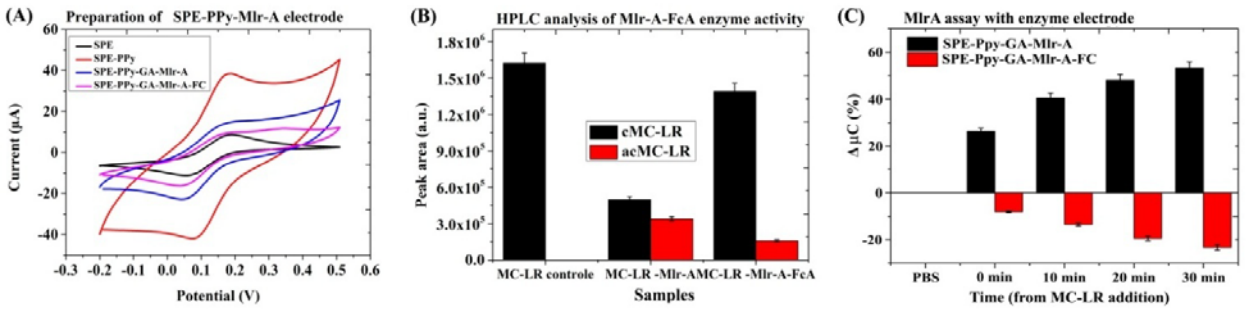

Fig. 16: A) FCN CV for prepared electrodes (SPE, SPE-Ppy, SPE-PPy-GA-MlrA and SPE-PPy-MlrA-FC). B) Enzyme activity of partially purified and unpurified MlrA and C) Electrochemical investigation of MlrA assay using SPE-PPy-GA-MlrA and SPE-PPy-MlrA-FC electrodes. Error bars show standard deviations of means for triplicate ($p = < 0.05$).

4. Discussion

The need for robust, on-site, and rapid water testing is widely accepted yet still hindered by the lack of enabling technology. In this study, we have developed a miniaturized electrochemical biosensor comprising a custom portable measurement platform and a combination of microelectrodes, each functionalized with a different probe and applying different electrochemical methods that complement each other.

Label-free EIS-based detection of MC-LR was enabled by simply incubating a sample for several minutes on an electrode functionalized with specific anti-MC-LR antibodies. The biosensor exhibited a high signal-to-noise ratio and a broad detection range of over five logarithmic concentrations. A calibration curve was constructed, achieving a detection limit at 3 ng/L (3 parts-per-trillion), superior to most reported sensors with only a few publications that demonstrate lower LODs [20], albeit at the cost of a considerably narrower dynamic range.

The performance of EIS-based biosensors is often limited by insufficient specificity due to non-specific adsorption and high false-positive rates. Therefore, we have coated the developed chip with a thin MC-LR layer, covalently immobilized via SAM, and constructed an electrochemical indirect competitive ELISA. After careful fine-tuning the reaction parameters and ensuring the stability of the electroactive substrate, we have applied a chronoamperometric measurement and obtained a specific cathodic current signal due to NAPQI electro-reduction, which was inversely proportional to the added MC-LR concentration, as expected.

The exceptional chemical and physical resistance of MC-LR, its persistence in the environment, and lack of distinct optical or electrochemical signature fuel the need for a specific biocatalytic recognition element that can provide a rapid and accurate diagnosis. It is widely accepted that probes with catalytic properties, e.g., enzymes, are instrumental in conferring biosensors with specificity and reusability. Therefore, the integration of MlrA as an active component in an enzyme-based biosensor for MC-LR detection is particularly promising and, to the best of our knowledge, has not been reported yet.

Here we developed an electrochemical biosensor employing MlrA as a probe for the detection of MC-LR from contaminated water. Detection of MC-LR can be achieved by

monitoring the potential during the enzymatic reaction and measuring the capacitive current of a MlrA-based composite electrode in the presence and absence of MC-LR. The feasibility of this newly developed electrochemical biosensor was demonstrated in the detection of MC-LR. Such a device may monitor enzymatic reaction in real-time and measure low concentration of MC-LR in the environment.

The developed integrated platform enabled measurements in highly complex matrices containing various aquatic bacteria, cell debris, and different biomolecules without any pretreatment. In comparison, previous studies have mostly reported on measurements conducted in buffers containing purified antigens [21,22] or, alternatively, filtered and centrifuged environmental water samples [23].

In addition, compared with other reported immunosensors for environmental applications, which usually rely on bulk electrodes in a conventional three-electrode setup [24], we have optimized microelectronic fabrication to generate a miniaturized, highly reproducible thin-film based electrochemical setup with an on-chip quasi-reference electrode that enables high-throughput measurements.

Most importantly, despite their complexity, detection of MC-LR from raw cyanobacteria cultures exhibited high specificity and the ability to discriminate between different cyanobacteria strains.

This new tool may largely contribute to an imminent water contamination crisis by enabling intensive testing on-site and alleviating most of the hurdles that plague current diagnostics. EIS-based devices may be further extended to allow automated continuous monitoring of surface water, which is highly desirable for novel on-site environmental diagnostics.

Finally, we would like to emphasize that the results of this study enticed water providers and companies such as Mekorot into forming new and promising collaborations. Based on this research, we have secured considerable funding from the Israeli Innovation authority to continue developing this biosensor and bring it to an advanced technology readiness level.

Publications, patents, and conference presentations.

Publications

[1] Abraham O. Ogungbile, Idan Ashur, Itzik Icin, Orr H. Shapiro, Sefi Vernick** (2021) Rapid detection and quantification of microcystins in surface water by an impedimetric immunosensors. *Sensors and Actuators B: Chemical, 2021, 348, pp 130687*

Patent applications

[2] Sefi Vernick, Abraham Ogungbile, Orr Shapiro, AN INTEGRATED MULTI-METHOD ELECTROCHEMICAL BIOSENSOR FOR RAPID-ON-SITE DETECTION AND/OR QUANTIFICATION OF SMALL MOLECULE TARGETS IN A SAMPLE. PCT/IL2021/051409

Conferences (Oral presentations)

[3] Development of MlrA enzyme- based electrochemical biosensor for real-time and direct detection of cyclic MC-LR. Dharanivasan Gunasekaran, Sefi Vernick. *240th Electrochemical Society (ECS) meeting, October 10-14, 2021*.

[4] Rapid Detection and Quantification of Microcystins in Surface Water by an Impedimetric Biosensor by Sefi Vernick, Abraham Ogungbile, Idan Ashur, Itzik Icin. *240th ECS meeting, October 10-14, 2021*.

[5] Electrochemical biosensor for rapid detection and quantification of Microcystins in surface waters. Sefi Vernick, Abraham Ogungbile, Idan Ashur, Itzik Icin. *Grand Water Research Institute (GWRI) annual meeting 2021, Technion, Israel.*

Bibliography

[1] D.M. Anderson, A.D. Cembella, G.M. Hallegraeff, Progress in Understanding Harmful Algal Blooms : Paradigm Shifts and New Technologies for Research , Monitoring , and Management, (2012). https://doi.org/10.1146/annurev-marine-120308-081121.

[2] Z. Svirčev, D. Drobac, N. Tokodi, B. Mijović, G.A. Codd, J. Meriluoto, Toxicology of microcystins with reference to cases of human intoxications and epidemiological investigations of exposures to cyanobacteria and cyanotoxins, Arch. Toxicol. 91 (2017) 621–650. https://doi.org/10.1007/s00204-016-1921-6.

[3] R. Wood, Acute animal and human poisonings from cyanotoxin exposure - A review of the literature, Environ. Int. 91 (2016) 276–282. https://doi.org/10.1016/j.envint.2016.02.026.

[4] I. Superiore, E. Testai, F.M. Buratti, E. Funari, M. Manganelli, S. Vichi, N. Arnich, R. Biré, V. Fessard, A. Sialehaamoa, Review and analysis of occurrence , exposure and toxicity of cyanobacteria toxins in food, (2016).

[5] A.D. Chatziefthimiou, R. Richer, J. Powell, J. Metcalf, Cyanotoxins as a potential cause of dog poisonings in desert environments, (2014) 8–11. https://doi.org/10.1136/vr.g3176.

[6] F. Gurbuz, J.S. Metcalf, A. Gul, G.A. Codd, Science of the Total Environment Analysis of dissolved microcystins in surface water samples from Kovada Lake , Turkey, Sci. Total Environ. 407 (2009) 4038–4046. https://doi.org/10.1016/j.scitotenv.2009.02.039.

[7] WHO, Guidelines for Drinking-water Quality SECOND ADDENDUM TO THIRD EDITION WHO Library Cataloguing-in-Publication Data, (2008) 17–19. https://doi.org/10.1016/S1462-0758(00)00006-6.

[8] I. Chorus, J. Bartram, Toxic Cyanobacteria in Water : A guide to their public health consequences , monitoring and management, 1999.

[9] U.P. App, Freshwater HABs Newsletter, (2017).

[10] M.P. Chatrathi, J. Wang, G.E. Collins, Sandwich electrochemical immunoassay for the detection of Staphylococcal enterotoxin B based on immobilized thiolated antibodies, Biosens. Bioelectron. 22 (2007) 2932–2938. https://doi.org/10.1016/j.bios.2006.12.013.

[11] I.I. Suni, Impedance methods for electrochemical sensors using nanomaterials, TrAC - Trends Anal. Chem. 27 (2008) 604–611. https://doi.org/10.1016/j.trac.2008.03.012.

[12] K. Hara, H. Arakawa, C. Dssc, S. Cell, D. Physics, K.M. Jeerage, R.D. Noble, C.A. Koval, M. Kouhnavard, N. Ahmad, L. Babak, V. Ghaffari, N. Chandra, D. Nath, H. Joon, W. Choi, J. Lee, 阻抗好书-Theory , Experiment , and, 2013. https://doi.org/10.1016/j.snb.2007.02.003.

[13] J. Yeh, B. Zhu, K.I.K. Wang, Z. Salcic, K. Kannappan, A. Partridge, Modelling diffusion impedance in the sensing of micron-sized particles, Sensors Actuators, B Chem. 237 (2016) 329–340. https://doi.org/10.1016/j.snb.2016.06.065.

[14] A. Lasia, Electrochemical Impedance Spectroscopy and its Applications - Andrzej Lasia - Google Books, 2014. https://books.google.com/books?id=lWEgBAAAQBAJ&printsec=frontcover&source=gbs_ge_summary_r&cad=0#v=onepage&q&f=false.

[15] M. Barreiros dos Santos, C. Sporer, N. Sanvicens, N. Pascual, A. Errachid, E. Martinez, M.P. Marco, V. Teixeira, J. Samiter, Detection of pathogenic Bacteria by Electrochemical Impedance Spectroscopy: Influence of the immobilization strategies on the sensor performance, Procedia Chem. 1 (2009) 1291–1294. https://doi.org/10.1016/j.proche.2009.07.322.

[16] L. Lu, G. Chee, K. Yamada, S. Jun, Electrochemical impedance spectroscopic technique with a functionalized microwire sensor for rapid detection of foodborne pathogens, Biosens. Bioelectron. 42 (2013) 492–495. https://doi.org/10.1016/j.bios.2012.10.060.

[17] Y. Hillman, J. Gershberg, D. Lustiger, D. Even, D. Braverman, Y. Dror, I. Ashur, S. Vernick, N. Sal-Man, Y. Wine, Monoclonal Antibody-Based Biosensor for Point-of-Care Detection of Type III Secretion System Expressing Pathogens, Anal. Chem. 93 (2021) 928–935. https://doi.org/10.1021/acs.analchem.0c03621.

[18] E.P. Randviir, C.E. Banks, Electrochemical impedance spectroscopy: An overview of bioanalytical applications, Anal. Methods. 5 (2013) 1098–1115. https://doi.org/10.1039/c3ay26476a.

[19] Lopes, I. C.; Santos, P. V. F.; Diculescu, V. C.; Peixoto, F. M. P.; Araujo, M. C. U.; Tanaka, A. A.; Oliveira-Brett, A. M., Microcystin-LR and chemically degraded microcystin-LR electrochemical

oxidation. *Analyst* **2012,***137* (8), 1904-1912.
[20] L. Ruiyi, X. Qianfang, L. Zaijun, S. Xiulan, L. Junkang, Electrochemical immunosensor for ultrasensitive detection of microcystin-LR based on graphene – gold nanocomposite / functional conducting polymer / gold nanoparticle /ionic liquid composite film with electrodeposition, Biosens. Bioelectron. 44 (2013) 235–240. https://doi.org/10.1016/j.bios.2013.01.007.
[21] C. Han, A. Doepke, W. Cho, V. Likodimos, A.A. De Cruz, T. Back, W.R. Heineman, H.B. Halsall, V.N. Shanov, M.J. Schulz, A Multiwalled-Carbon-Nanotube-Based Biosensor for Monitoring Microcystin-LR in Sources of Drinking Water Supplies, (2013) 1807–1816. https://doi.org/10.1002/adfm.201201920.
[22] W. Zhang, M.B. Dixon, C. Saint, K.S. Teng, H. Furumai, Electrochemical Biosensing of Algal Toxins in Water: The Current State-of-the-Art, (2018). https://doi.org/10.1021/acssensors.8b00359
[23] F. Tan, N.M. Saucedo, P. Ramnani, A. Mulchandani, Label-Free Electrical Immunosensor for Highly Sensitive and Speci fi c Detection of Microcystin-LR in Water Samples, (2015). https://doi.org/10.1021/acs.est.5b01674
[24] V. Vogiazi, A. De La Cruz, S. Mishra, V. Shanov, W.R. Heineman, D.D. Dionysiou, A Comprehensive Review: Development of Electrochemical Biosensors for Detection of Cyanotoxins in Freshwater, ACS Sensors. 4 (2019) 1151–1173. https://doi.org/10.1021/acssensors.9b00376